Optical Engineering, Volume 58, Issue 2, 2019, Article number 025103
DOI:10.1117/1.OE.58.2.025103

Comparison of empirical and predicted ultraviolet aircraft signatures

Itor James,[a*] Mark Richardson,[a] Eoin O'Keefe,[b]
[a]Cranfield University, Defence Academy of the UK, Shrivenham, Wiltshire, UK, SN6 8LA
[b]QinetiQ, Cody Technology Park, Farnborough, Hampshire, UK, GU14 0LX

Abstract. In light of the potential threat to aircraft from missiles using Ultra Violet (UV) wavebands, it is important to understand the signature of an aircraft and how this can be predicted. This study compares empirical UV signature data to modelled data from CAMouflage Electro-Optical SIMulation (CAMEOSIM) to determine how well the contrast between the object and the background can be predicted using local knowledge of the atmosphere. CAMEOSIM uses the standard MODerate resolution atmospheric TRANsmission (MODTRAN) model to estimate the radiative transfer through the atmosphere. Both MODTRAN and CAMEOSIM are well validated in visible and infrared wavebands and MODTRAN can accurately predict UV radiative transfer. Unfortunately, the work so far has concentrated on bulk transfer to describe the sky background in the UV where the aircraft scene is typically a negative contrast 'hole' in a positive sky background. Importantly, path-to-path scattering is a key consideration in this scene since it is this that will tend to blur the edges of an object and reduce the contrast associated with it. A developed understanding of the limitations is required. It was determined that prediction was possible up to ranges of 5km. The local visibility (in km) was required for this prediction.

Keywords: ultraviolet, aircraft, signature, prediction, modelling, atmosphere.

***Itor James, E-mail: i.james@cranfield.ac.uk

1 Introduction

CAMEOSIM is a tool, developed by Lockheed Martin UK, that produces digitally modelled scenes that are radiometrically accurate in various wavebands and for various backgrounds including land (foliage) and aerial (sky). It uses MODTRAN, which is a standard tool, developed by the US Air Force and Spectral Sciences Inc., that is used to predict the radiative transfer of energy through the atmosphere. It has been shown to be accurate at predicting the radiation

Published by SPIE. This is the Author Accepted Manuscript issued with: Creative Commons Attribution Non-Commercial License (CC:BY:NC 4.0).
The final published version (version of record) is available online at DOI:10.1117/1.OE.58.2.025103. Please refer to any applicable publisher terms of use.

received at the surface of the earth through many studies [1]–[4]. Current limitations in how MODTRAN calculates scattering will influence the accuracy of using it for the determination of negative contrast signatures of targets in the UV. The contrast is defined here as the difference in pixel value recorded between the sky background and the target, this is normalised to the highest value (relevant) pixel in the scene. This gives a range of contrast values between +1 (bright target and dark background) and -1 (dark target and bright background) with 0 as the zero contrast case (target and background having the same pixel value). The path-to-path scattering is detailed in Figure 1 below and is the scattering of energy between optical paths, it is important to consider when scattering can increase the signal observed rather than scattering merely causing losses, which no longer need to be considered. Therefore, to understand whether signature predictions can be made, some comparison of the predictions to empirical data are required. In the military context, it is important to understand how the signature of an aircraft target varies with range so that it is known at what range a missile can detect the target aircraft. Various factors within the control of the aircraft designer will affect this aircraft signature, such as the surface reflective and radiative properties. This understanding allows tactical mitigation of effective missile ranges to be accomplished (such as flying higher or further from a known threat). A typical aircraft scene will be a bright UV sky background with a negative contrast (silhouette) from the aircraft. A requirement was produced to understand two aspects of this problem:

1. To what degree of accuracy MODTRAN could predict the contrast between the sky background and an aircraft (or other) object in the foreground
    a. For a single object against a uniform background
    b. At various ranges
2. Whether there were important effects not modelled in MODTRAN (such as the path-to-path scattering) that would adversely affect the ability to undertake such predictions
    a. What importance they had in the accuracy of the model
    b. Whether they could be replicated in another way

An experiment to test this was devised so that MODTRAN predicted data (obtained using CAMEOSIM to model an extended target object) could be compared to empirical data taken from aircraft and ships (some of which was obtained before the modelling took place). This will be described below.

2 CAMEOSIM data capture

CAMEOSIM is a software tool that can represent large and complex shapes embedded in realistic camouflage environments for military studies. The physical atmospheric radiation transfer is calculated for all of the single transmission points to all of the receiving points using MODTRAN to produce images with a full radiometric treatment of the scene. CAMEOSIM's primary use is to investigate camouflage patterns against realistic foliage and terrain across the Electro-Optical (EO) spectrum consistent with the wavelength limitations imposed by MODTRAN (0.2 to 100 μm). Therefore, CAMEOSIM should be able to represent the UVA and UVB parts of the Electro-Magnetic (EM) spectrum (0.28 to 0.4 μm) as well as further out to the visible and IR. Owing to this expected MODTRAN accuracy, as well as availability and familiarity, CAMEOSIM was chosen as tool to investigate UV transmission for various target scenes. CAMEOSIM can predict the full object signature where MODTRAN will predict the atmospheric extinction over a single path. This is completed through the consideration of multiple radiation paths. The predicted CAMEOSIM data was to be compared to empirical data to determine the accuracy of the predicted contrast at various ranges.

A scenario was created in CAMEOSIM. The target object was to be represented as follows:

Table 1 CAMEOSIM cases modelled

	0% UV reflective object (referred to as black)		100% UV reflective object (referred to as white)	
	5m x 5m area	15m x 15m area	5m x 5m area	15m x 15m area
280-400nm waveband	5km visibility 23km visibility 'Maritime' visibility	5km visibility 23km visibility 'Maritime' visibility	5km visibility 23km visibility 'Maritime' visibility	5km visibility 23km visibility 'Maritime' visibility
280-500nm waveband	5km visibility 23km visibility 'Maritime' visibility	5km visibility 23km visibility 'Maritime' visibility	5km visibility 23km visibility 'Maritime' visibility	5km visibility 23km visibility 'Maritime' visibility

The parameters were chosen for the following reasons:

Size – This represents a typical approximate aircraft observable plan area (5m x 5m) and the approximate plan area of the Naval ship, that had already been recorded (15m x 15m).

UV Reflectivity – Both extremes of the reflectivity were required to ensure that both the desired skin treatment effect (white) and the current target status (black) were represented. The UV reflectivity of typical paints is approximately 0% and the skin treatment was as close to 100% reflective as possible. The skin treatment was chosen to be as representative as possible to highly reflective UV paint which was developed in parallel to this work.

Wavebands – Two wavebands were chosen to represent the potential waveband for a UV missile seeker. The first is a classic UVA and UVB waveband (approximately 280-400nm), the second is a slightly expanded waveband including UVA, UVB and some blue (approximately 280-500nm). This is owing to the assumption that a missile making use of the 'UV' would use UVA and UVB, to obtain a higher bandwidth and would not include UVC (<280nm) since this is not well transmitted through the atmosphere. The expansion into the blue is controversial in that it may increase the potential to have a positive contrast between the aircraft and the sky in the visible portion of the waveband and a negative contrast in the UV portion of the waveband at the same time, this may integrate to zero signal at the target without suitable care.

Attenuation – The atmospheric attenuation values chosen are representative of a typical high visibility day (23km) and a low visibility day (5km). These are standard definitions within MODTRAN and well used values in other studies. A further attenuation was chosen to represent the maritime case and used on all the other data sets. The maritime transmission includes more aerosol (from the water spray close to the water surface) and, therefore, related scattering effects. The effect on the UV may not be as high owing to the larger water particle sizes and the relationship between wavelength, scattering and particle size [5]–[7].

The background irradiance was a standard illumination based on a typical UK spring/autumn day (15.5 W/sr/m2) and the atmosphere chosen was 'standard' (a parameter within MODTRAN) with other parameters varied as above. The objects were placed at low altitudes in the standard atmosphere and observed co-planar. The ground was removed to limit any effect of reflections from the ground. All the data was normalised to represent contrast between the object and the sky background since this is a result which should be independent of sky irradiance. The UV signature is defined as a silhouette against the sky background where the UV reflectivity is zero, i.e. the object tends to absorb all the radiation impinging on it. If all the incident UV radiation

can be absorbed in the absorptive case, the magnitude of the contrast between the object and the sky will vary between zero and one depending only on the reflectivity of the object to the UV radiation. The magnitude of the contrast will reduce with increasing range as the background radiation from the sky is scattered into the path between the observer and the object as shown below.

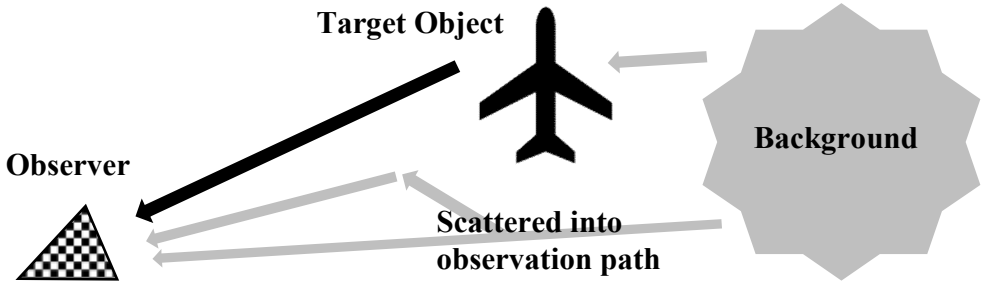


Figure 1 UV scattering around object showing signature

Assuming a constant atmosphere, this propensity to scatter is only dependent on the wavelength of the radiation [5] (and not the intensity of the radiation), i.e. this scattering is independent of the sky background irradiance. The background irradiance (in the UV) is produced by scattering in the higher atmosphere, this is the same mechanism by which the target signature is modified at range. However, if a constant atmosphere is assumed over the target to observer variation, then the level of scattering will not be increased if the background intensity is increased. For example, if the atmosphere remains constant between dawn and midday, the background intensity will increase but the amount of scattering for each path at different times of day will remain the same. Given this, the contrast variation is expected to be independent of sky irradiance value (where the atmosphere is constant) and so the only data shown is the contrast normalised to the background level. This is broadly equivalent to the Minimum Resolvable Temperature Difference (MRTD) that is used to describe the sensitivity of InfraRed (IR) detectors without reference to the absolute temperature of background or object.

In all cases in the CAMEOSIM simulations, the number of pixels which were required to have their irradiance computed for an observer was to be minimised for speed, therefore, a square object was chosen, and the extent of the background was minimised. A further experimental requirement was to ensure that the angular size of the object was consistent for all data so frames at different ranges were comparable. In CAMEOSIM, data was run for a 100% reflective (white)

object against a sky like background case and a 0% reflective (black) object against a sky like background case. In both cases, the full height and width of the output scene was 64x64 pixels, the middle 32x32 pixels always represented the target object and the outer pixels represented the background. These can be seen conceptually in Figure 2 below. The range is variable.

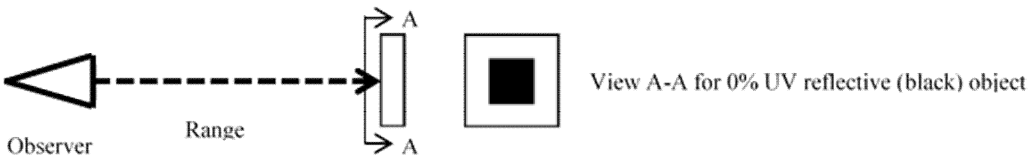


Figure 2 CAMEOSIM model visualisation (black object)

The view 'A-A' of the target object and background in Figure 2 shows a black square (the target) surrounded by a white border (the background). Irrespective of target physical size (5x5m or 15x15m) or range from the observer to the object, the output image, representing the scene viewed by the observer, was arranged to be consistently a 64x64 pixel image with a central square target of 32x32 pixels. In this way, direct comparisons can be made between different ranges without having to apply scaling to the images in post processing. It is important to note that the intensity of the pixels at the range of the observer through the atmosphere is represented by the contrast stored (the pixel value) after the loss to scattering and transmission. For example, the 0% UV reflective 'black' target against the sky background for a MODTRAN sky prediction commensurate with a 5km visibility atmosphere, the 280-400nm waveband and at 0km range to the observer is shown (as in view A-A in Figure 2) below in Figure 3. Figure 3 also shows the similar 100% UV reflective 'white' target case on the right. The white case is lower (but not zero) contrast where the black case is higher contrast.

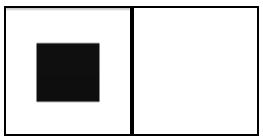


Figure 3 'Black' air target (left) & 'white' (right), 5km visibility, 280-400nm waveband

As the object moves away, the contrast between the object and the background reduces (in both the black and the white cases). Various attenuation cases were run (5km and 23km visibility in

the air cases and a sea/maritime visibility) as well as for two wavebands. In all cases, a sweep of ranges was computed from 0km to 30km in 500m steps (with finer resolution at short ranges.

2.1 Modelled data

Of the 64x64 pixel data for each observer range, a horizontal slice of data was taken at the vertical half way point (vertical pixel 32) so that a clear representation of the central region of the target was taken. This slice included all 64 horizontal pixels, it assumes no vertical variation of the target. This slice can then be compared to other slices at other ranges. The first comparison was the arbitrary pixel intensity units. These can be seen in Figure 4 and Figure 5. The 'black' case can be seen in Figure 4 each line on the chart shows a reading at a different range from the observer to the target. Each line represents the central slice of pixels from the results detailed above, with the horizontal pixel numbers 0-16 and 48-64 representing the background pixel value (irradiance) and the central horizontal pixels (17-47) represent the target pixel values. As the range increases between the observer and the target, the contrast (difference in the target and background pixel values) decreases, this can be seen in the variability between the different lines on the charts. This shows that the central block has a negative contrast compared to the background. The x-axis value shows the horizontal pixel number and the arrow shows the reducing negative contrast as the range between the target and observer increases.

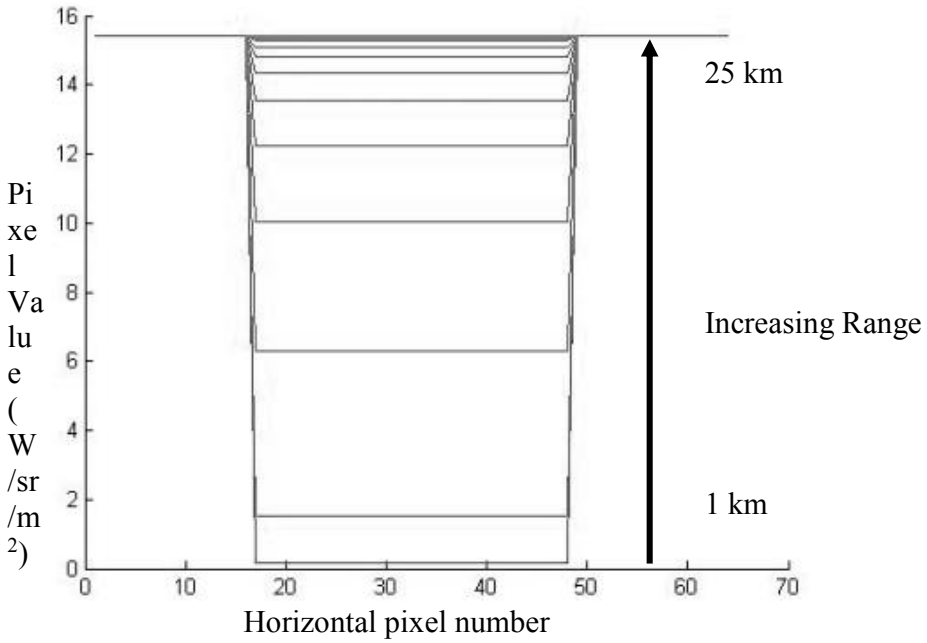


Figure 4 'Black' case showing contrast changing at various ranges

In the case below, showing the ‘white’ case, the same pattern is observed of a reduction in the value of contrast (this time positive) compared to the background as range increases. The positive value is representative of the total reflection of the sky background and the smaller range between the object and the observer. The value of the pixels on the target object are variable (manifesting as noise on the horizontal lines) owing to them representing reflections of the sky background (which has some random fluctuations in it), this is since the object is 100% reflective and diffuse rather than radiating at the same level as the background. Its appearance will be dominated by reflections of the sky behind the observer. Further, these values are normalised to allow comparison with the ‘black’ case above. The variation in contrast for the white case, seen below, is somewhat counterintuitive but can be explained by the limited method by in which the calculation was performed. The background, to limit computing load, was fixed at a given radiation at all times just further away than the furthest target object (30km) and directly behind the observer. It was a small cell of atmosphere that had an irradiance associated with it. As the white object approaches the range of the background the contrast will reduce as the path lengths seen by the observer from the ‘background’ and the target object become more

similar. This limitation on the method means that the data for the black case is more likely to be empirically matched than the white case.

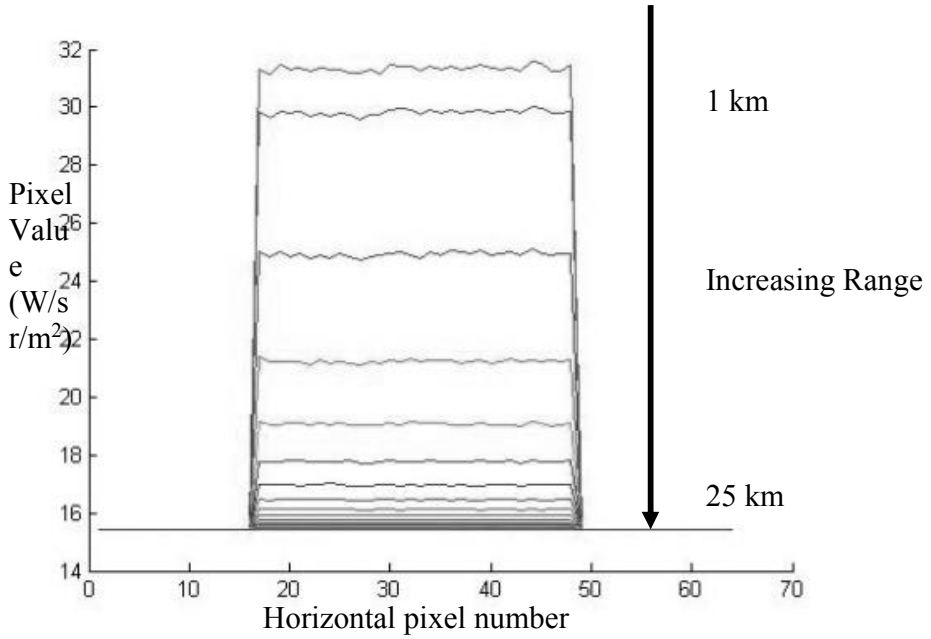


Figure 5 'White' case showing contrast changing at various ranges

These data are better represented as a curve plotting a single contrast value from each frame (or slice) against the range at which that reading was taken. This is the information that follows in the plots. In all cases, the average contrast level of the central slice (vertical pixel 32, horizontal pixel 16-48) of the target object was taken as the single representative value of contras, with the contrast values being normalised to +1 at the zero range case (this means the effect of range on the positive contrast and negative contrast data can be compared). It should not be taken to imply that the absolute value of contrast is similar.

2.1.1 'Black' maritime aerosol attenuation cases (maritime visibility atmosphere using MODTRAN data)

The plot below shows the data as range (km) on the x-axis and the normalised contrast for all the range cases on the y-axis. This contrast data is taken directly from the CAMEOSIM produced data described in the previous section but groups different cases so that the variation in range of the contrast can be better seen. It shows the two-waveband cases as different lines. The two wavebands chosen were 280nm-400nm and 280nm-500nm as described earlier. It is interesting to note that the two-waveband cases are very similar in absolute contrast levels for various

ranges. This would not, necessarily, be expected owing to the increased propensity of UV light to scatter within a scene compared to blue (visible) light [5] in clear conditions, UV light (300nm) would be expected to scatter three times more strongly than blue light (400nm) in the atmosphere. Whilst Mie scattering would dominate in occluded conditions (such as with fog), in clear conditions, the Rayleigh scattering should ensure that the UV would scatter more. Rayleigh scattering increases as the wavelength decreases, therefore, it could be expected that the UV would scatter more. This could mean lower contrast as the target silhouettes become filled in with scattered UV radiation. Whilst this is the case, the difference is not as pronounced as the author expected it to be and is certainly not as pronounced as the three times more scattering might suggest it would be.

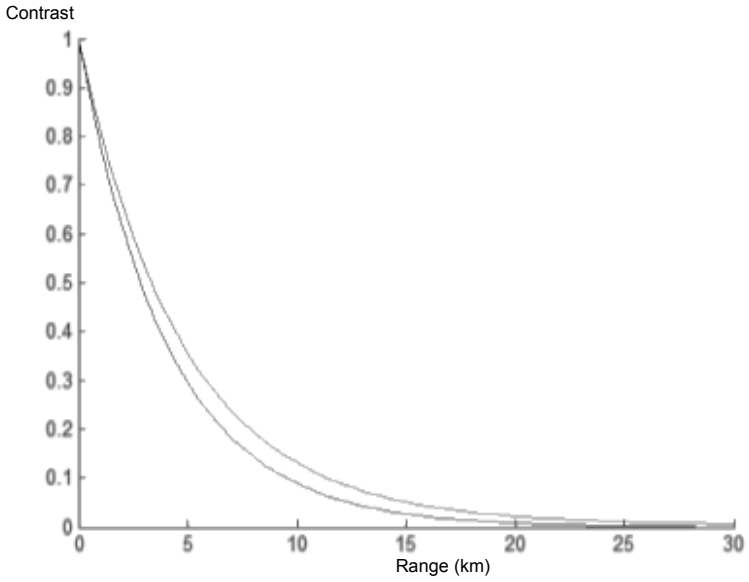


Figure 6 'Black' maritime aerosol attenuation case, 280-400nm (left) & 280-500nm (right)

This data is visibly equivalent to the exponential extinction curves relating range to attenuation which can be obtained directly from MODTRAN. However, it has been recalculated for an extended object in the UV portion of the spectrum to represent the typical aircraft seen against a sky background. This has not knowingly been completed before.

2.1.2 'Black' and 'white' air aerosol attenuation cases (5km visibility atmosphere using MODTRAN data)

A similar set of data is plotted for the air aerosol attenuation cases with 5km visibility in Figure 7 below. In this case, the 'black' case is compared to the 'white' case using the same data as presented in Figure 4 and Figure 5. Here, the 'white' case has been made positive (and normalised) for ease of comparison. This shows that the two absolute contrast changes with range are very similar in nature (albeit different in magnitude). Owing to the high level of similarity observed and the limitations associated with the modelling, no more consideration of the white cases will be undertaken in this paper. Further work will be required to understand the different absolute values of various UV reflectivities.

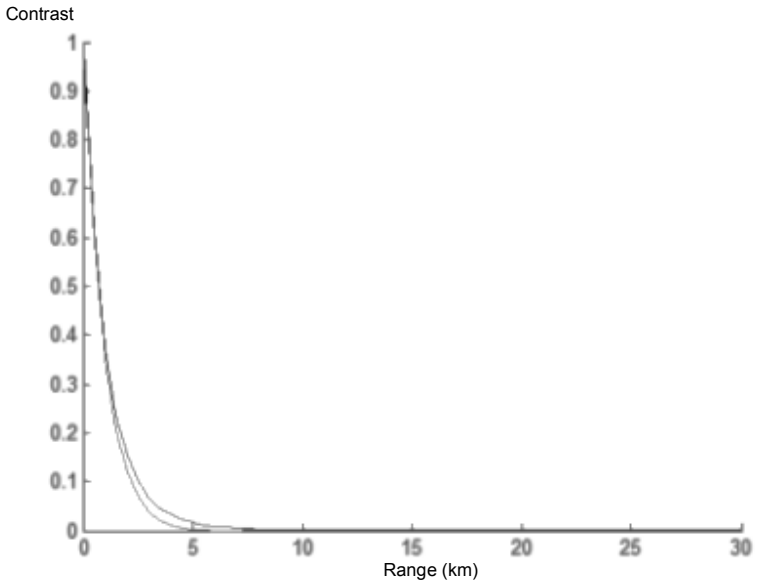


Figure 7 'Black' (left) and 'white' (right) air aerosol attenuation cases, 5km visibility, 280-500nm waveband

2.1.3 Other 'black' cases

Combining the 'black' data from the two different air aerosol attenuation cases, as well as both maritime aerosol attenuation cases for comparison is presented in this section. The 'white' data has no further analysis owing to its perceived similarity in range variance to the 'black' case and the fact that the black cases was immediately available for comparison to empirical data.

2.1.4 Air aerosol attenuation cases (5km and 23km visibility atmospheres)

Figure 8 shows all the 'black' air aerosol attenuation data in one plot. This shows the significant difference between the 5km visibility case (bad visibility day) and the 23km visibility case (good visibility day) along with the much smaller variation for the different UV wavebands. It would be expected that the zero-contrast level for the UV data would be similar to the zero-contrast level for the visible waveband (the visibility limit) and that the 280-500nm case would be more like the visible than the 280-400nm case. It is possible that the visibility limit would be at shorter range in the UV than the visible but this should be proved. The expected similarity between the UV wavebands and the visible extinction point is borne out in the plot for short ranges, in that the zero-contrast UV point appears to occur at a similar range to the maximum visibility values. For example, the 5km visibility case gives a zero-contrast UV range at between 4km and 5km. However, there is more UV contrast than would be expected at long ranges in the 23km visibility case, the UV zero-contrast point is predicted to be beyond 30km. The reason for this is unknown and it was not expected that the range at which contrast could be detected in the UV, where more scattering occurs, would appear to be greater than in the visible waveband.

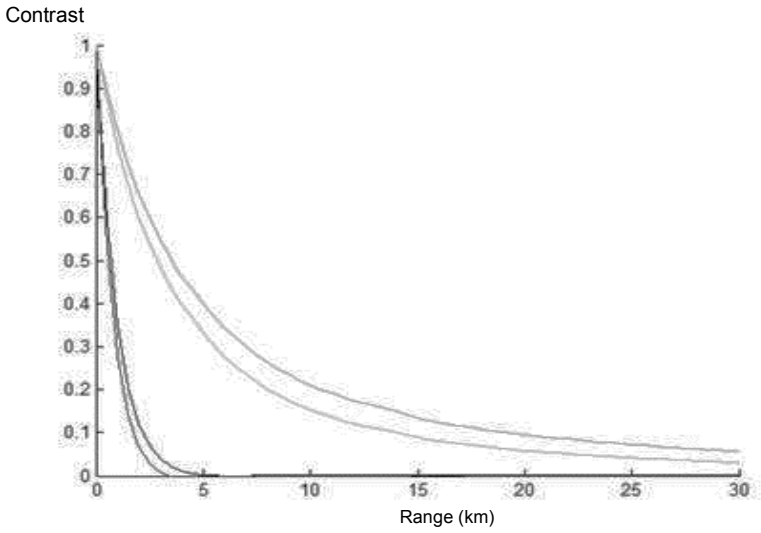


Figure 8 'Black' air cases; 5km visibility 280-400nm (first, left to right), 5km visibility 280-500nm (second), 23km visibility 280-400nm (third), 23km visibility 280-500nm (fourth)

Figure 8 also shows that there is little predicted contrast difference between the two wavebands in the 5km visibility cases but a greater predicted contrast difference (almost 0.1) in the 23km

visibility cases. This is an interesting phenomenon and may be attributable to the 23km visibility cases containing different sized aerosols that may differentially affect the shorter wavelengths of light in the 280-400nm case. It may also be that the proportional difference is similar but the magnitude of the difference is, therefore, higher for the longer range cases.

2.1.5 Maritime aerosol attenuation (maritime visibility atmosphere)

A similar analysis approach is presented for the maritime cases below although only one atmospheric attenuation model was used, referred to as 'maritime'. This is shown in Figure 9, which indicates a similar trend to that seen in the air 23km visibility cases. The predicted contrast differences are less than in the 23km visibility air case and the zero-contrast level, defined as the point where the contrast is below 0.001 occurs at a shorter range, approximately 23km to 30km.

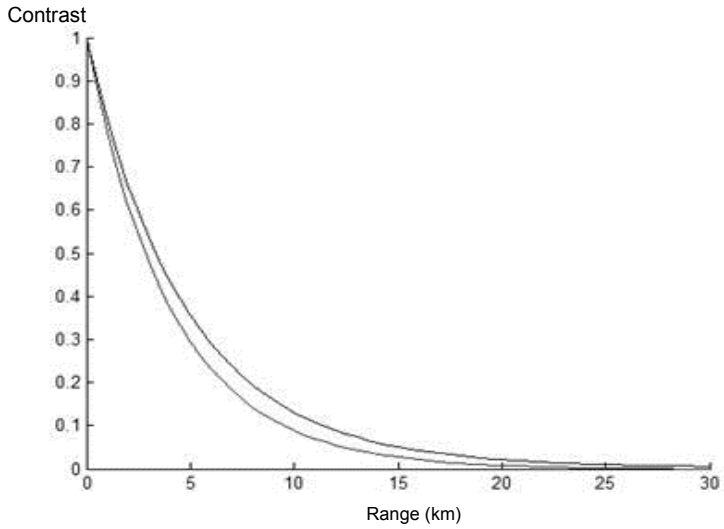


Figure 9 'Black' maritime aerosol attenuation cases; maritime visibility 280-400nm (left), maritime visibility 280-500nm (right)

2.1.6 All visibility atmospheres

The extinction prediction data for all the 'black' cases (air and maritime aerosol attenuation) can be seen in
Figure 10 below.

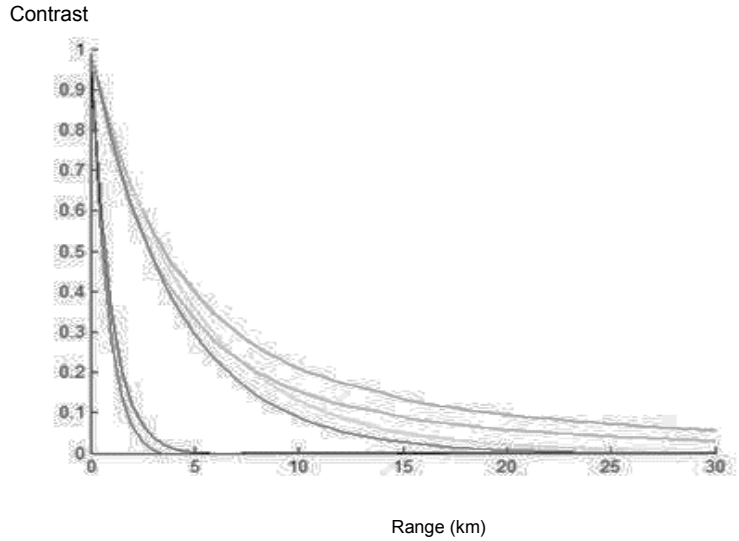


Figure 10 All 'black' air and maritime aerosol attenuation cases; 5km air visibility 280-400nm (first, left to right), 5km air visibility 280-500nm (second), maritime visibility 280-400nm (third), maritime visibility 280-500nm (fourth), 23km air visibility 280-400nm (fifth), 23km air visibility 280-500nm (sixth)

The plot indicates that the air 23km visibility cases and the maritime visibility cases are similar, particularly at ranges less than approximately 5km. The data shown in this chart can now be compared to empirical data to test the hypothesis that it can be used for contrast prediction.

3 Empirical contrast

This section will provide explanation of the method used to gather empirical UV contrast data at various ranges as well as the empirical contrast values obtained.

In most cases, the actual irradiance values of the sky background were also obtained but these have not been used in this study. Further work may examine whether background intensity has a significant effect on the contrast prediction although it is not expected to and it is assumed that it does not to allow for comparison of the black and white cases. For the UV scene described, a negative contrast target, the signature is created by a physical obstruction of the sky background. If it is assumed that the intensity of the UV background does not influence the propensity of the background UV to scatter (there is no mechanism by which it should), then the contrast reduction over range will be limited by the same properties whatever the background intensity. There may

yet be correlation between a bright UV background and the scattering properties of the atmosphere that would influence the contrast measured but this may not imply a direct causation. The sea and air cases will, again, be dealt with separately and combined at the end. It is assumed that the paint on both the aircraft measured and the ship is Titanium Dioxide (TiO_2) based and is therefore approximately 0% reflective (black) in the UV. It may be much higher than this in some empirical cases as shown in Figure 11. The first case is the maritime case; this provides explicit detail on the methods used, saving repetition in the other cases.

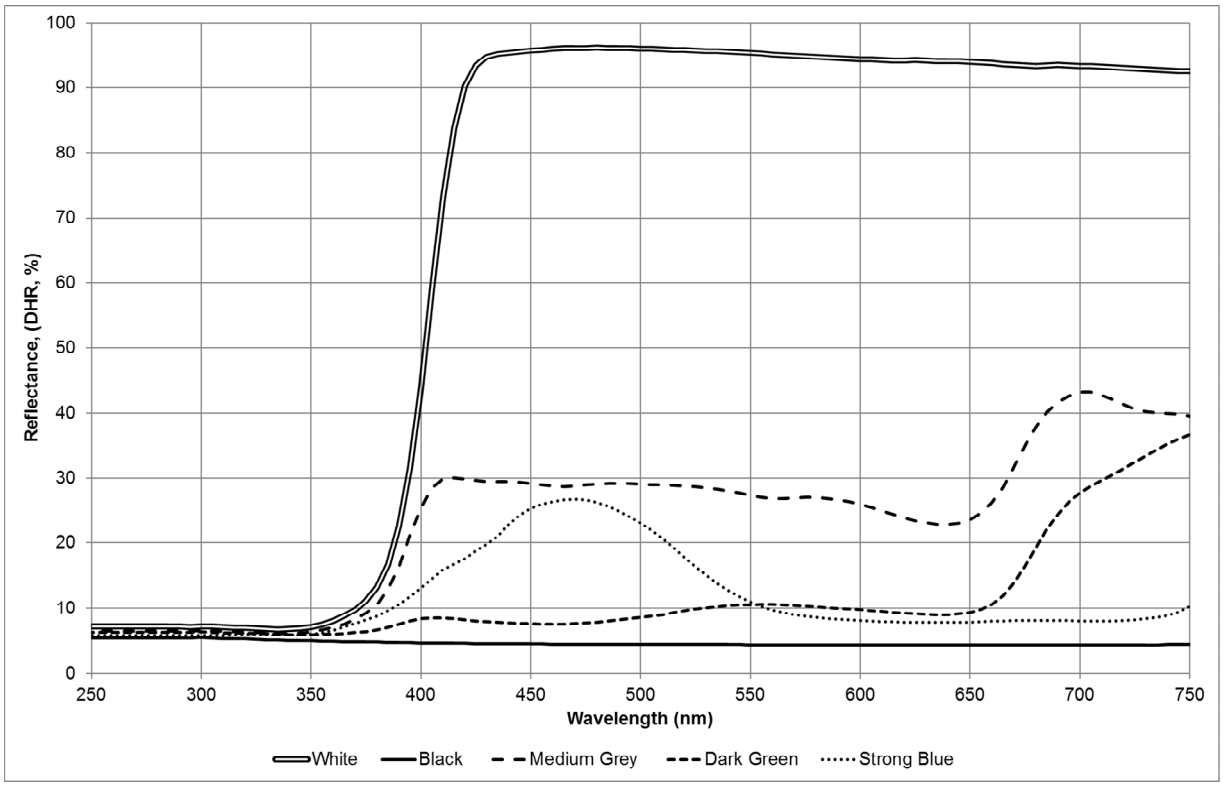


Figure 11 Some empirical TiO_2 based paint reflectivities for different wavelengths (visible colour differences shown)

3.1 Maritime cases

Figure 12 shows a screenshot of a Matlab tool being used to interrogate pixel values for the image of the ship on the left of the figure. The small grey rectangle superimposed on the image is magnified in the inset window; this displays the pixel locations and values for this region.

The image shows a ship sailing away from Portsmouth (UK) taken using a full spectrum converted 12Mpixel Si CMOS DSLR with 105mm UV quartz lens and UV transmitting filters. It

represents the 280-500nm waveband although with a limited responsivity and as an uncalibrated detector. As discussed in the previous section, the difference in contrast owing to the two different wavebands is minimal and so they will be assumed to be approximately the same for ease of comparison with the empirical data. The range of the ship was determined using a public transponder system that can be interrogated, via the internet, in near real-time. The ship has an approximately 15mx15m aft aspect which is the aspect observed in the images included. These images were kindly taken and supplied by the STAAR labs at QinetiQ, UK.

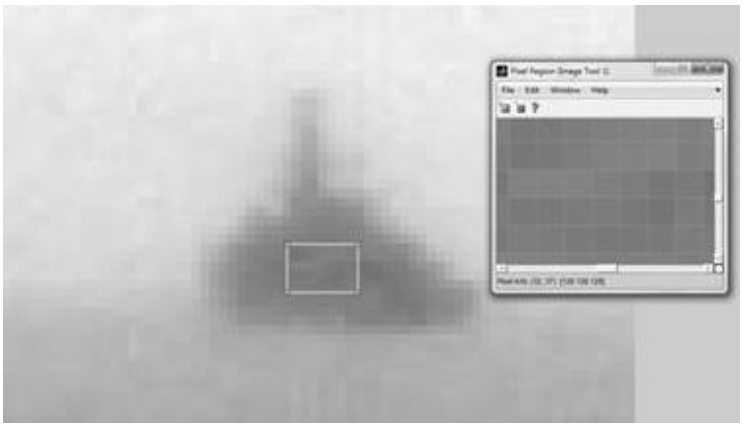


Figure 12 Empirical maritime case (ship pixels highlighted), 5km range

Using the pixels within the region highlighted in the Figure 12 and taking the average pixel values of all of them, gave a typical black level for the ship at this range. A smaller or larger region could have been chosen but the largest rectangle possible was chosen that excluded any background or transitional (edge) pixels*.

Using this tool, the average pixel value for the region highlighted was calculated to be 125.39. The pixel values can range from zero (black) to 256 (white) in the black and white images that were used for this study. Next, a comparable region of the sky was required to enable calculation of the contrast between the ship and the sky. As shown in Figure 13 a region was chosen as far away as possible from the ship.

* Great care should be taken in doing this in Matlab since Matlab expects inputs for averaging and mathematical operation of matrices in the form (ROW, COLUMN). Traditional pixel locations (including those in the shown Matlab tool) use the form (COLUMN, ROW). It is not known why such an inconsistency exists within a single tool but it can be worked around with prior knowledge and care.

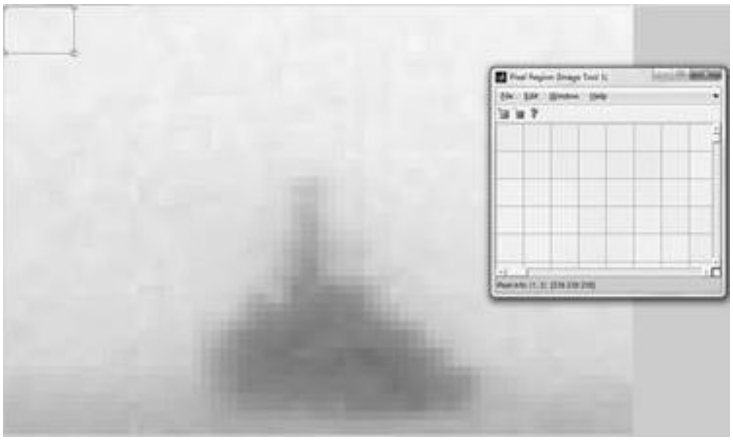


Figure 13 Empirical maritime case (far sky pixels highlighted), 5km range

Taking the average pixel value for this region gives a value of 238.5. This implies the contrast at 5km is 0.47 (or 47%). Repeating this for an image taken at 10km range as shown in Figure 14 is shown below.

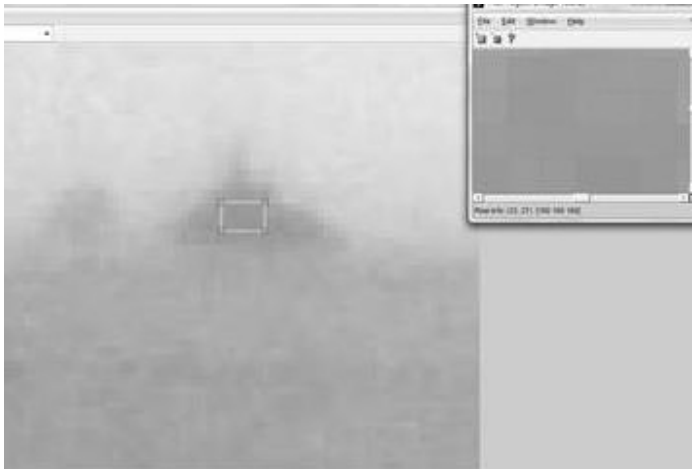


Figure 14 Empirical maritime case (ship pixels highlighted), 10km range

On closer inspection, it was deduced that the contrast level would only be of practical use in the region around the ship. Any comparison of ship to sky contrast within a missile would likely happen close to the ship to detect a difference and, therefore, an object. Further, the angle of view between the ship and the far patch of sky could be very different which may mean that the sky in this region is artificially bright or dark compared to that near the ship. Finally, a far patch

of sky may be outside of the Field of View (FOV) of any observing optical system, such as a missile seeker. Therefore, repeating for an 'average' nearby patch of sky compared to the ship gives the 'near' cases (compared to the 'far' cases, which refer to the comparison to the corner of the image already presented). An example is shown in Figure 15 below. The observed contrast will be compared between the near and far cases.

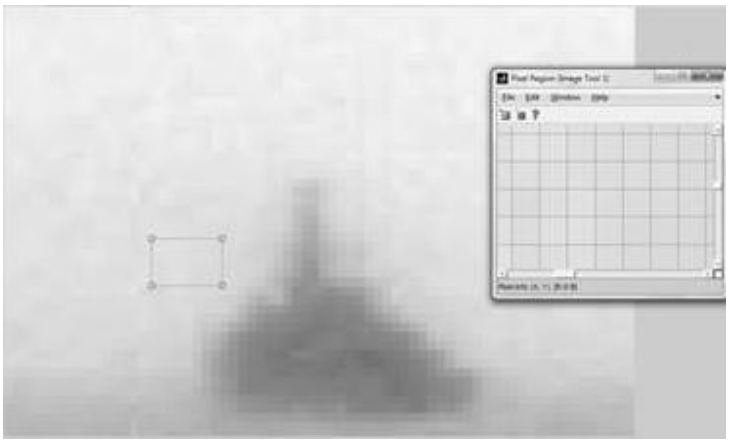


Figure 15 Empirical maritime case (near sky pixels highlighted), 5km range

3.2 Sea summary

In summary, the ship pixel level did change with range as shown in Table 2, it tended to become lighter (transitioning from pixel level 0 to 256) as range increased, as would be expected. The contrast was calculated from two patches of sky background, one 'near' and the other 'far' from the ship and the mean of both cases was also taken for each range, this data is shown in Table 2.

Table 2 Empirical contrast data, sea summary

	5km	**10km**	**15km**
Ship Blackness Level	125.39	154.57	162.25
Far Contrast	0.47	0.32	0.27
Near Contrast	0.43	0.27	0.15
Mean Contrast	0.45	0.30	0.21

It is likely that the ‘near’ case is a better consideration since the contrast will be calculated from physically adjacent points in the missile seekers considered. Further, the far corner of the image is at a very different viewing angle than the direct line to the ship. In general, the contrast levels are similar in both the near and far sky cases and a mean can be calculated. It is curious that although the contrast decreases with range that the blackness level of the ship pixels increases slightly as the range increases. The reason for this is not known although it may be some auto-exposure in the camera processing. If it is a camera setting, particularly an automatic one, it is likely that this will affect the background as well as the target object and may not have a large effect on the contrast.

3.3 Air cases

Another set of data points were taken using the same camera observing aircraft displaying at the 2018 Farnborough airshow. This was observed on the 20th July 2018 from a location within the QinetiQ site at Farnborough. Multiple aircraft were present and flew at different ranges. Whilst a lot of data exists, much is repeated in that the aircraft range does not often change. The purpose of this study is to compare the range vs contrast prediction and empirical data so limited data points were chosen representing different size aircraft at different ranges.

The same technique was applied to the air cases as to the maritime cases above with the added calculation of the range from the camera to the target aircraft. This was accomplished through open source data [8], [9] describing the aircraft present and by calculating the range through knowledge of the size of the camera detector (23.1mm x 15.4mm) along with the focal length of the lens used (105mm).

3.3.1 Harrier (AV8B)

The aircraft can be seen in Figure 16 below.



Figure 16 Harrier UV photo (full frame)

In Figure 17 below, the measurements of the Harrier (in pixels) is shown as well as the full frame length (in pixels) at the base of the picture are superimposed over Figure 16.



Figure 17 Harrier UV photo image measurement (beam)

Reference [8] indicates this Harrier (AV8B) is 14.53m long, which gives the range that this photo was taken as 1921m. This was calculated using trigonometry, the dimension of the object

on the frame (159.03 pixels), the full frame pixel width (4608 pixels) and the field of view (12.6^{o}) of the camera. Below is the frame taking samples of the aircraft signature in Figure 18 and the sky background in Figure 19, both these figures are zoomed in versions of Figure 16.

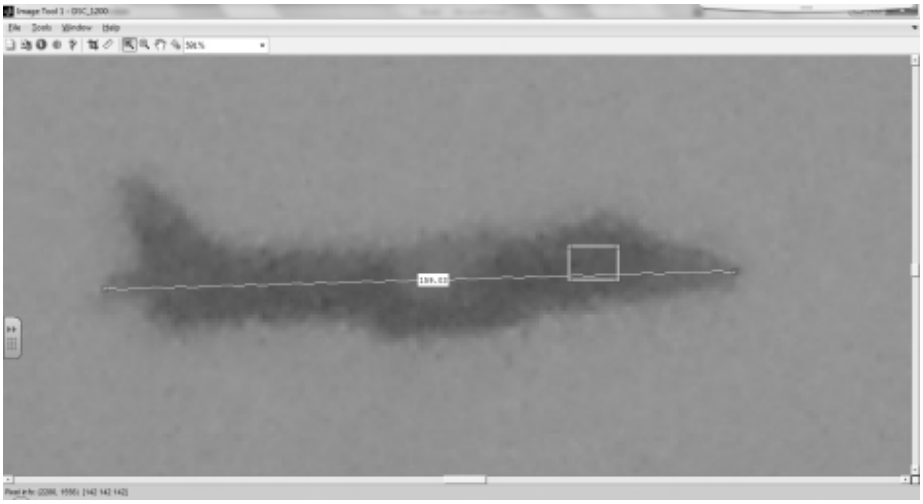


Figure 18 Cropped Harrier UV photo (aircraft pixels highlighted)

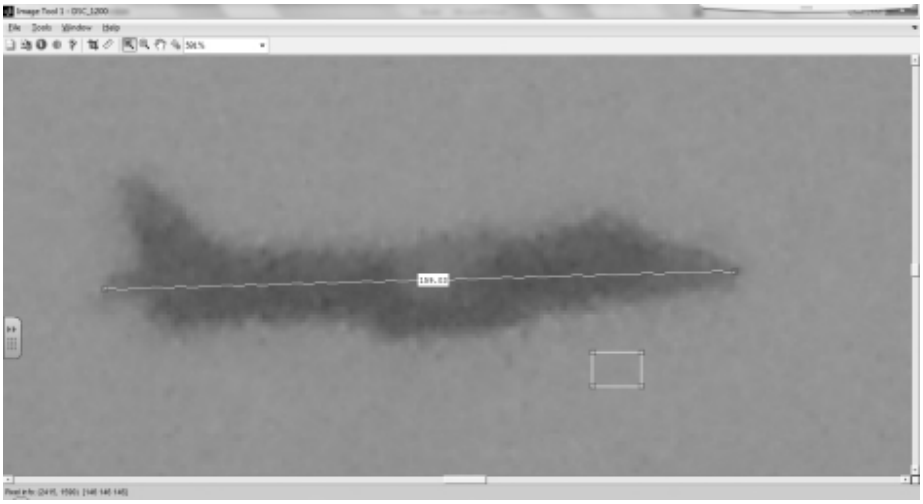


Figure 19 Cropped Harrier UV photo (near sky pixels highlighted)

The process is repeated for the far sky value patch above and the contrast in both the near sky and far sky contrast cases is calculated as in the maritime cases. This gives the following data:

Near contrast = 0.36

Far contrast = 0.38

3.4 Air summary

The following table gives a summary of all of the air cases recorded, the ranges and the aircraft chosen. They have been re-ordered into increasing range for each aircraft. The average contrast has also been included, calculated from the near and far sky cases as an arithmetic mean.

Table 3 Air summary cases

	GR7				A350			
	Underside	Underside	Beam	Beam	Topside	Beam	Beam	
Range (m)	189	1721	1921	2413	2345	4363	5550	
Near Contrast	0.74	0.51	0.36	0.42	0.24	0.24	0.19	
Far Contrast	0.74	0.52	0.38	0.44	0.24	0.24	0.20	
Mean Contrast	0.74	0.51	0.37	0.43	0.24	0.24	0.20	
	T129 ATAK		**727-200**				**EA300 Blade**	
	Beam	Beam	Nose	Beam	Beam	Beam	Underside	Beam
Range (m)	2013	2316	724	1327	2671	5108	951	1719
Near Contrast	0.40	0.38	0.68	0.47	0.32	0.20	0.59	0.32
Far Contrast	0.41	0.37	0.68	0.46	0.34	0.19	0.60	0.35
Mean Contrast	0.40	0.37	0.68	0.47	0.33	0.20	0.60	0.33

The general trend is for the contrast to decrease with range; this is as predicted and as expected.

4 Results

The following sections will detail the comparison of the predicted contrast levels (from CAMEOSIM) to the empirical data. Both the air and maritime cases are compared to the predictions.

4.1 Comparison to predictions (maritime cases)

Figure 20 shows the comparison of the empirical maritime cases to various CAMEOSIM predictions of contrast.

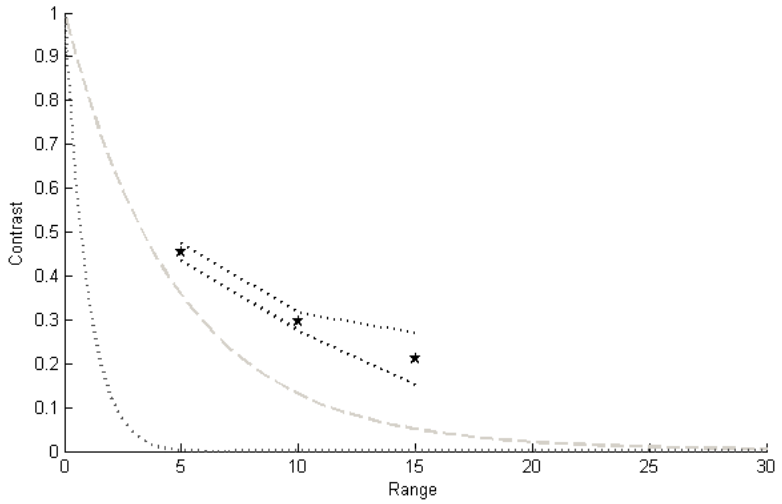


Figure 20 Comparison of empirical sea data to CAMEOSIM predictions; 'black' air case, 280-500nm (black dotted line); 'black' maritime case, 280-500nm (grey dashed line); empirical maritime case 'near' sky (top black dotted line); empirical maritime case 'far' sky (bottom black dotted line); mean empirical maritime case (black stars)

Clearly, the limited empirical maritime data does not closely match the predicted CAMEOSIM data either for the 5km visibility 'black' air extinction case or for the maritime visibility 'black' extinction case. The 'near' empirical case, representing the contrast with a nearby patch of sky, is much closer to the CAMEOSIM maritime prediction above and would be a much more sensible measure of contrast than the far or mean contrast cases. It is not known why there is a discrepancy in the maritime case that is different to the air case, it is expected that this may be aerosol based. However, it is also counterintuitive that the empirical data would be higher contrast than the CAMEOSIM predictions given that the CAMEOSIM takes no account of path-to-path scattering and the additional reduction in contrast this will provide. It may be the case that the empirical data was taken on a particularly bright or dry (with less aerosol) day which the MODTRAN maritime extinction cases were not representative of.

The difference shown is large in terms of percentage error (using the CAMEOSIM data as the baseline to calculate this from), however, the magnitude of the systematic error is 0.08 (8%) to 0.14 (14%) in contrast (the mean is approximately 11%), this is independent of range for the cases shown.

4.2 Comparison to predictions (air cases)

Plotting the average contrast (mean of near sky and far sky cases) along with the furthest and shortest visibility predictions (for air and sea) gives the chart shown in Figure 21 below.

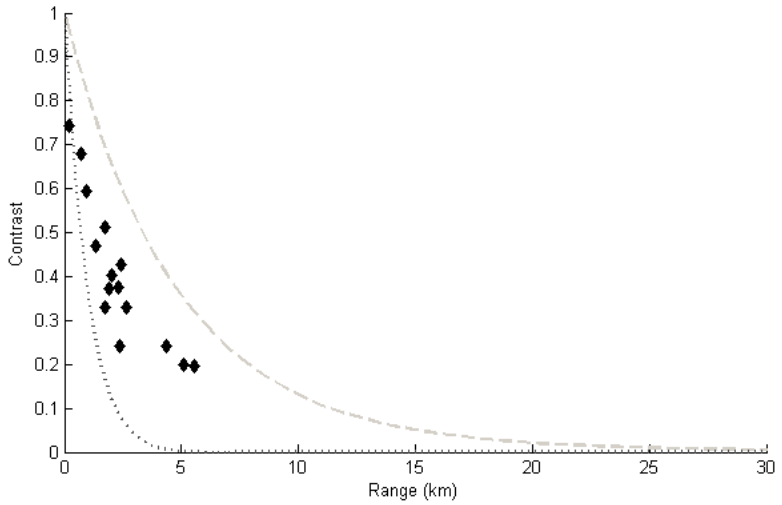


Figure 21 Comparison of empirical air data to CAMEOSIM predictions; 'black' air case, 280-500nm (dark grey dotted line); 'black' maritime case, 280-500nm (light grey dashed line); empirical air cases (black diamonds)

A least squares trend line for this empirical data was calculated and added to the chart in green and shown in Figure 22. This was fixed to have the following characteristics; crosses the y-axis at 1 (i.e. the contrast is normalised to 1), an exponential decay, extrapolated to meet the x-axis.

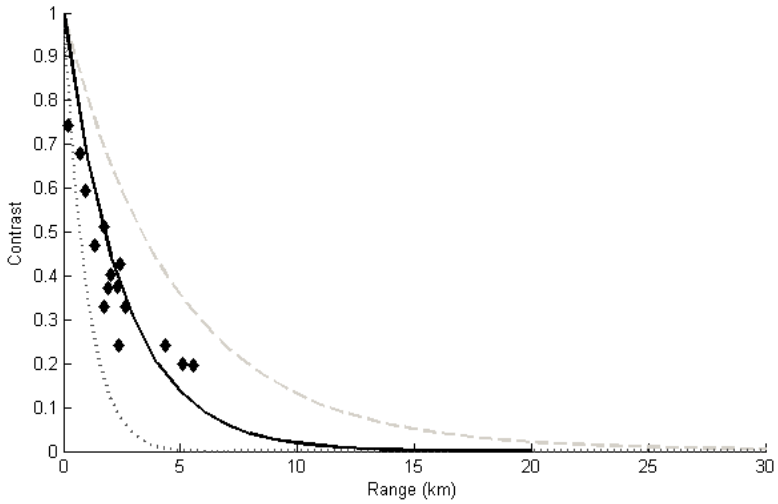


Figure 22 Comparison of empirical air data to CAMEOSIM predictions; 'black' air case, 280-500nm (dark grey dotted line); 'black' maritime case, 280-500nm (light grey dashed line); empirical air cases (black diamonds); exponential best-fit trendline for empirical data (black line)

The Excel best-fit algorithm minimises the total magnitude of the error from the trendline. The extinction point predicted by this trendline[†] is approximately at 13-15km, which fits in reasonably with the measured visibility on the day of between 8km and 17km (with a mean of 14km)[‡]. This visibility data was taken by Farnborough airfield and obtained from [10].

The exponential best fit line is also very similar to the predicted extinction from a single point MODTRAN run. The data for 14km visibility in the 200-500nm waveband is shown in Figure 23 below, it is expected that this will be very similar to the 280-500nm line owing to the very limited atmospheric transmission at the shorter wavelength end of this band. The chart is a repeat of Figure 22 above with the addition of a dotted black line with square markers (MODTRAN 14km visibility in 200-500nm) which shows the similarity between this and the empirical exponential best fit line which is solid black.

[†] The extinction was approximated as the range at which the contrast dropped below 2%. A common approximation for visible acuity is the 2% contrast point and this was used in the absence of knowledge about the detector.

[‡] The recorded data was 2x readings at 17km and 1x at 8km for approximately 3 hours during which data was gathered, the mean is therefore 14km

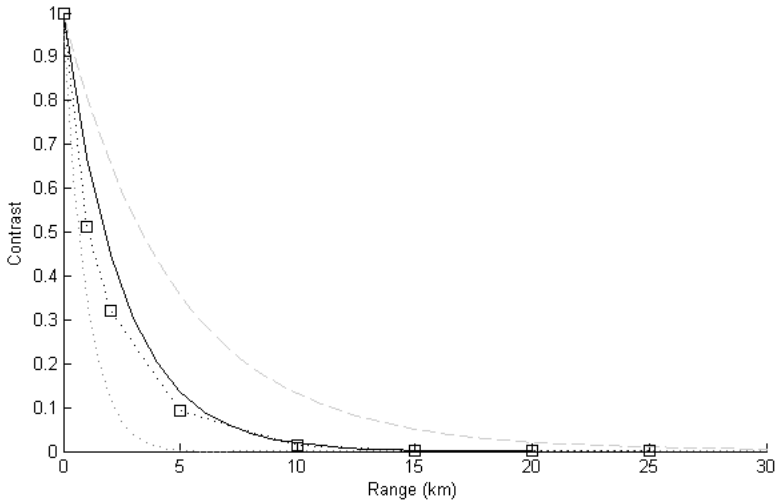


Figure 23 As Figure 22 with additional MODTRAN 14km visibility (200-500nm) as a black dotted line with square markers to compare to solid black line (exponential best fit to empirical air data)

It appears that the exponential best fit can be considered as an approximation to both a CAMEOSIM and MODTRAN based extinction case, for this atmosphere. This is owing to the similarity of the shape of the predicted lines and the best fit line.

Further work has shown that the curves shown in the figures above from the CAMEOSIM predictions and the empirical data can also be approximated as exponential decay lines. This should not be surprising given the concept of the optical depth describing the atmospheric attenuation. To illustrate this, Figure 22 is repeated below as Figure 24 with exponential decay approximations to the two CAMEOSIM prediction lines and the empirical best fit line to the empirical data included and represented as plots of small circles. The equations of the lines are in the form e^{kx} where x is range (in km) and k is a constant, the values of the constants are given in Table 4. A way to characterise the exponential curves was required, this was chosen to be the range at which the contrast was 0.02 or 2%. This value has been chosen since this is a common visual acuity measure for contrast. The exponential curves created to approximate the CAMEOSIM predictions were chosen to have a contrast value of 0.02 (≈0) at approximately 23km and 5km. These correspond to the stated visible band visibility of those atmospheric conditions in the MODTRAN data used (23km for the maritime and 5km for the air). However, the exponential approximations and the CAMEOSIM predictions do not align precisely, in all cases, the exponential approximations show higher contrast.

Using the range at which contrast decays to 0.02 as a characteristic means any exponential approximation to the CAMEOSIM prediction can be made for this common atmospheric characteristic. The visible band visibility is commonly measured and recorded and is therefore a useful characteristic of the atmosphere that is being observed through. These predictions are shown below with the following line details: 'black' air case, 280-500nm (dark grey dotted line), exponential approximation to the 'black' air case (dark grey dots); 'black' maritime case, 280-500nm (light grey dashed line), exponential approximation to the 'black' maritime case (light grey dots); empirical air cases (black diamonds); exponential best-fit trendline for empirical air data (black solid line), exponential approximation to the empirical air cases best-fit trendline (black dots)

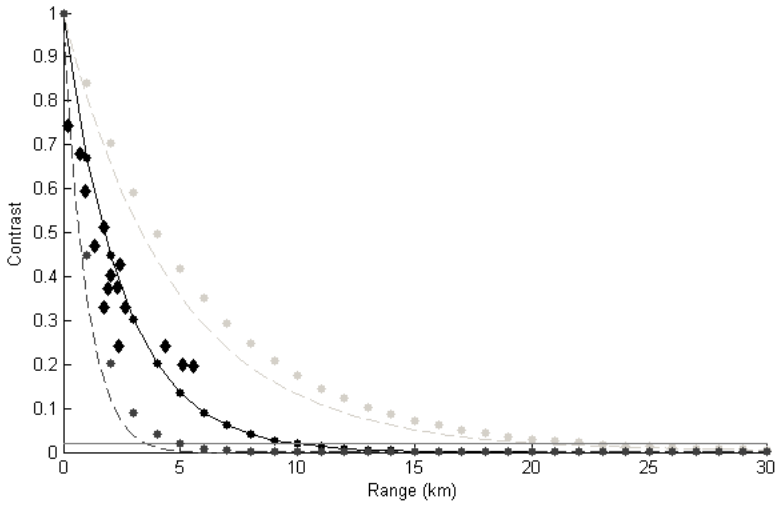


Figure 24 Comparison of empirical air data to CAMEOSIM predictions and exponential predictions (2%)

However, it would be better to more accurately match the curves that the CAMEOSIM modelling predicts. By using the range at which contrast decays to 0.005 (or 0.5%), better matches to the CAMEOSIM data can be obtained. This data is shown in Figure 25 below. Two further lines are included as black dashed lines which are the exponential curves for the 8km and 17km visible band visibility cases (i.e. exponential lines that give a contrast of 0.005 at 8km and 17km). These values of visible band visibility were those recorded at the Farnborough Airshow by the airport on the day that the data was recorded. The curve representing the best fit line for the empirical measurements crosses the 0.005 line at ≈13km which is close to the mean (14km) of the various visibility measurements recorded at Farnborough.

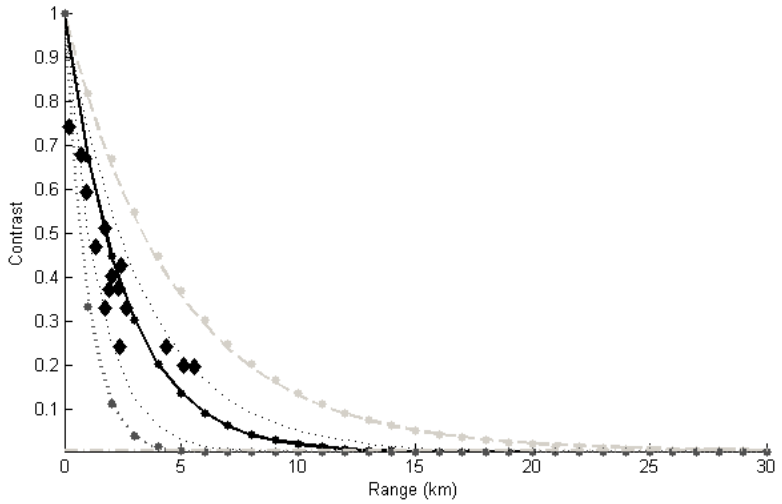


Figure 25 Comparison of empirical air data to CAMEOSIM predictions and exponential predictions (0.5%)

Figure 25 shows the following data: 'black' air case, 280-500nm (dark grey dotted line), exponential approximation to the 'black' air case (dark grey dots); 'black' maritime case, 280-500nm (light grey dashed line), exponential approximation to the 'black' maritime case (light grey dots); empirical air cases (black diamonds); exponential best-fit trendline for empirical air data (black line), exponential approximation to the best-fit trendline for the empirical air data (black dots); 8km visibility MODTRAN data exponential approximation (left hand black dashed line); 17km visibility MODTRAN data exponential approximation (right hand black dashed line)

Table 4 Exponential decay constants (k) for various lines

	Black maritime case (5km visibility)	8km visibility line	Empirical data (best fit) line	17km visibility line	Black maritime case (23km visibility)
Constant (k) 2%	-0.8	-0.5	-0.3	-0.24	-0.175
Constant (k) 0.5%	-1.1	-0.7	-0.3	-0.32	-0.23

It is interesting to note all of the empirical air results fit within the bounds described by the 8km and 17km visible band visibility approximations (using the 0.5% approximation). The accuracy of this prediction should be further investigated with more data. It is also interesting that the least

squares best fit exponential line is equivalent to the 14km visibility (using the 0.5% approximation) which is similar to the mean visibility on the day.

5 Discussion and conclusion

The implication of the data shown is that it is possible to predict the bulk contrast of an aircraft against the sky using an existing tool such as MODTRAN (within CAMEOSIM) for short ranges, up to approximately 3-5km. The effective range for some missiles is similar in magnitude and so this process could be used to predict the contrast of an object for a typical engagement in the UV assuming that the visibility is known for the atmosphere. It has been shown that an exponential decay function is a valid approximation to the predictions from CAMEOSIM and that this may also be used for signature prediction too if the visible band visibility characteristic of the atmosphere is known or can be predicted. However, the contrast limit that is required is lower than that for visible acuity. The reason for this is likely to be the lower contrast expected in the UV (owing to stronger atmospheric scattering) rather than the ability of UV detectors to perceive lower levels of contrast than the human eye in the visible waveband. Further validation of this is required for more atmospheres and using more data.

However, care must be taken since it has also been shown that the visibility model that is used has a significant effect on the predicted level of contrast. The similarity between the prediction for a 23km visibility atmosphere and a maritime atmosphere is shown in

Figure 10 but the 5km visibility prediction is very different. This should be expected but care must be taken to use an appropriate atmospheric model and suitable visibility value when predicting contrast.

More data will be required to prove that the background irradiance has no effect on the contrast level and to understand whether long-range predictions are valid. More data will also inform whether any sort of sea-based prediction can be made from CAMEOSIM and MODTRAN and whether any linear adjustment is required in the maritime case.

It is significant that the ‘in path’ scattering, which was not expected to be well considered in MODTRAN (and therefore CAMEOSIM), is not adversely affecting the ability of tools to predict the contrast at short ranges or it is having an offsetting effect. It was expected that an adjustment would be required to account for this. It appears, from this initial analysis, that the

contribution of this effect is negligible in a real atmosphere at short ranges. More work is required to understand why this is the case and at what range this effect becomes important.
The edge blurring of the images seen, particularly in the maritime case, is a function of this 'in path', or path to path scattering. It is possible that this could be crudely represented in a prediction tool using an edge blurring algorithm that was limited to the extent of the original object i.e. that the edge of the black object got brighter but the edge of the sky did not get darker. A modified jpeg or similar edge-blurring algorithm, which became more severe with range, may be able to approximate this but more work would be required to determine if this was valid. Interestingly, the empirical contrast level in the centre of the object did not appear to be altered by this edge blurring and it was mainly the edges of the object that were affected. This may be the reason that the limited consideration of the 'in path' scattering did not influence the measurements of contrast since these were taken in the centre of the objects. If the overall contrast of the complete object were taken, it is possible that this edge blurring would affect the contrast recorded.

In conclusion, although more data is required to further verify this, it seems that it is likely to be possible to predict the UV contrast of an aircraft and sky scene at short ranges either through complex tools such as CAMEOSIM and MODTRAN or approximately using an exponential decay characterised by the visibility (in the visible wavelengths) recorded or expected on the day. This visibility data is readily available and is predictable by meteorological experts and models. It is also possible that the actual, radiometric, aircraft signature can be predicted using the advanced model CAMEOSIM (with MODTRAN data) assuming the same knowledge of the atmospheric conditions including the background conditions.
This ability to predict UV scenes was not known to be possible previously and was not expected to be the case.

References

[1] L. Smith, M. Richardson, and R. Walmsley, "Comparison of MODTRAN5 to measured data in the UV band," in *SPIE Security + Defence*, 2013, vol. 8898, p. 88980F.

[2] G. E. Bodeker, R. L. Mc Kenzie, and R. L. Mckenzie, "An Algorithm for Inferring Surface UV Irradiance Including Cloud Effects," *Repr. from J. Appl. Meteorol.*, vol. 35, no. 10, 1996.

[3] S. Yeşilkaya, M. , Özsaraç and M. Y. E. S, "Cloud modeling in the infrared band," in *2013 21st Signal Processing and Communications Applications Conference*, 2013.

[4] P. G. Cox, R. G. Driggers, M. Spie, J. Leachtenauer, R. Vollmerhausen, F. Belvoir, and D. A. Scribner, "Targeting and intelligence electro-optical recognition modeling: a juxtaposition of the probabilities of discrimination and the general image quality equation," *Opt. Eng.*, vol. 37, no. 3, p. 789, Mar. 1998.

[5] A. Bucholtz, "Rayleigh-scattering calculations for the terrestrial atmosphere," *Appl. Opt.*, vol. 34, no. 15, pp. 2765–2773, 1995.

[6] A. A. Burns and P. Valley, "Aircraft Defense System Against MANPADS with IR/UV Seekers," US 7523692 B1, 28-Apr-2009.

[7] P. Weihs, A. R. Webb, S. J. Hutchinson, and G. W. Middleton, "Measurements of the diffuse UV sky radiance during broken cloud conditions," *J. Geophys. Res.*, vol. 105, no. D4, pp. 4937–4944, 2000.

[8] Wikipedia, "Harrier Jump Jet." [Online]. Available: https://en.wikipedia.org/wiki/Harrier_Jump_Jet.

[9] I. Source, "Nikon D3100 Review." [Online]. Available: https://www.imaging-resource.com/PRODS/D3100/D3100A.HTM. [Accessed: 12-Aug-2018].

[10] rp5.co.uk, "Weather archive in Farnborough (airport)." [Online]. Available: http://rp5.co.uk/Weather_archive_in_Farnborough_(airport). [Accessed: 12-Aug-2018].

[11] James I., "Comparison of empirical and predicted UV aircraft signatures (Invited Paper)" in Technologies for Optical Countermeasures XV, edited by David H. Titterton, Robert J. Grasso, Mark A. Richardson, Proceedings of SPIE Vol. 10797 (SPIE, Bellingham, WA, 2018) 10797-15.

Itor James is a part time PhD researcher at the Defence Academy of the United Kingdom since 2013, he also works at the UK Defence Science and Technology Laboratory (Dstl). He received his MEng degree in Engineering (Mechanical) from the University of Warwick in 2003. His current research interests include optical missile guidance and UV aircraft signatures. He is a member of SPIE.

Professor Mark Richardson is the Pro-Vice-Chancellor – Cranfield Defence and Security and is a member of the University Executive. Mark has been at Cranfield University at the Defence Academy of the United Kingdom, Shrivenham since 1989 and has previously been the Director of Defence and Security Technology, the Director of Research and the Head of the Centre of Electronic Warfare, Information and Cyber.

Mark's specialisation is in the field of Electronic Warfare (EW) particularly Electro-Optics and Infrared (EO&IR). His main teaching duties are on postgraduate courses, in particular Defence Technology, Guided Weapons and Electronic Warfare MSc's. He also lectures in the United States on various EW and EO&IR courses and seminars, and has taught EW and EO&IR to the Australian Technical Staff Officers Course at the Australian Defence Force Academy in Canberra on six occasions. He has also taught EO&IR Electronic Warfare at the Finnish School of Military Electronics in Riihimaki. His research work is in the fields of Infrared Signature Simulation & Modelling and EO&IR Countermeasures. He has written over 300 classified and unclassified papers on these subjects, and holds a Classified Patent on a novel Infrared Camouflage Material. He is the editor and principal author of a book on battlefield surveillance technology and has acted as a consultant and defence analyst, on numerous occasions, to both the UK Ministry of Defence and commercial industry.

Biographies and photographs for the other authors are not available.

Caption List

Figure 1 UV scattering around object showing signature
Figure 2 CAMEOSIM model visualisation (black object)
Figure 3 'Black' air target (left) & 'white' (right), 5km visibility, 280-400nm waveband
Figure 4 'Black' case showing contrast changing at various ranges
Figure 5 'White' case showing contrast changing at various ranges

Figure 6 'Black' maritime aerosol attenuation case, 280-400nm (left) & 280-500nm (right)
Figure 7 'Black' (left) and 'white' (right) air aerosol attenuation cases, 5km visibility, 280-500nm waveband
Figure 8 ‘Black’ air cases; 5km visibility 280-400nm (first, left to right), 5km visibility 280-500nm (second), 23km visibility 280-400nm (third), 23km visibility 280-500nm (fourth)
Figure 9 ‘Black’ maritime aerosol attenuation cases; maritime visibility 280-400nm (left), maritime visibility 280-500nm (right)
Figure 10 All ‘black’ air and maritime aerosol attenuation cases; 5km air visibility 280-400nm (first, left to right), 5km air visibility 280-500nm (second), maritime visibility 280-400nm (third), maritime visibility 280-500nm (fourth), 23km air visibility 280-400nm (fifth), 23km air visibility 280-500nm (sixth)
Figure 11 Some empirical TiO_2 based paint reflectivities for different wavelengths (visible colour differences shown)
Figure 12 Empirical maritime case (ship pixels highlighted), 5km range
Figure 13 Empirical maritime case (far sky pixels highlighted), 5km range
Figure 14 Empirical maritime case (ship pixels highlighted), 10km range
Figure 15 Empirical maritime case (near sky pixels highlighted), 5km range
Figure 16 Harrier UV photo (full frame)
Figure 17 Harrier UV photo image measurement (beam)
Figure 18 Cropped Harrier UV photo (aircraft pixels highlighted)
Figure 19 Cropped Harrier UV photo (near sky pixels highlighted)
Figure 20 Comparison of empirical sea data to CAMEOSIM predictions; ‘black’ air case, 280-500nm (black dotted line); ‘black’ maritime case, 280-500nm (grey dashed line); empirical maritime case ‘near’ sky (top black dotted line); empirical maritime case ‘far’ sky (bottom black dotted line); mean empirical maritime case (black stars)
Figure 21 Comparison of empirical air data to CAMEOSIM predictions; ‘black’ air case, 280-500nm (dark grey dotted line); ‘black’ maritime case, 280-500nm (light grey dashed line); empirical air cases (black diamonds)
Figure 22 Comparison of empirical air data to CAMEOSIM predictions; ‘black’ air case, 280-500nm (dark grey dotted line); ‘black’ maritime case, 280-500nm (light grey dashed line); empirical air cases (black diamonds); exponential best-fit trendline for empirical data (black line)
Figure 23 As Figure 22 with additional MODTRAN 14km visibility (200-500nm) as a black dotted line with square markers to compare to solid black line (exponential best fit to empirical air data)
Figure 24 Comparison of empirical air data to CAMEOSIM predictions and exponential predictions (2%)
Figure 25 Comparison of empirical air data to CAMEOSIM predictions and exponential predictions (0.5%)

Table 1 CAMEOSIM cases modelled
Table 2 Empirical contrast data, sea summary
Table 3 Air summary cases
Table 4 Exponential decay constants (k) for various lines



https://dspace.org/

Comparison of empirical and predicted ultraviolet aircraft signatures

James, Itor; Richardson, Mark A.; O'Keefe, Eoin

2019-02-09
SPIE - International Society for Optics and Photonics
https://doi.org/10.1117/1.OE.58.2.025103
James I, Richardson M, O'Keefe E. (2019) Comparison of empirical and predicted ultraviolet aircraft signatures. Optical Engineering, Volume 58, Issue 2, February 2019 Article number 025103

Downloaded from a DSpace repository. https://dspace.org/